

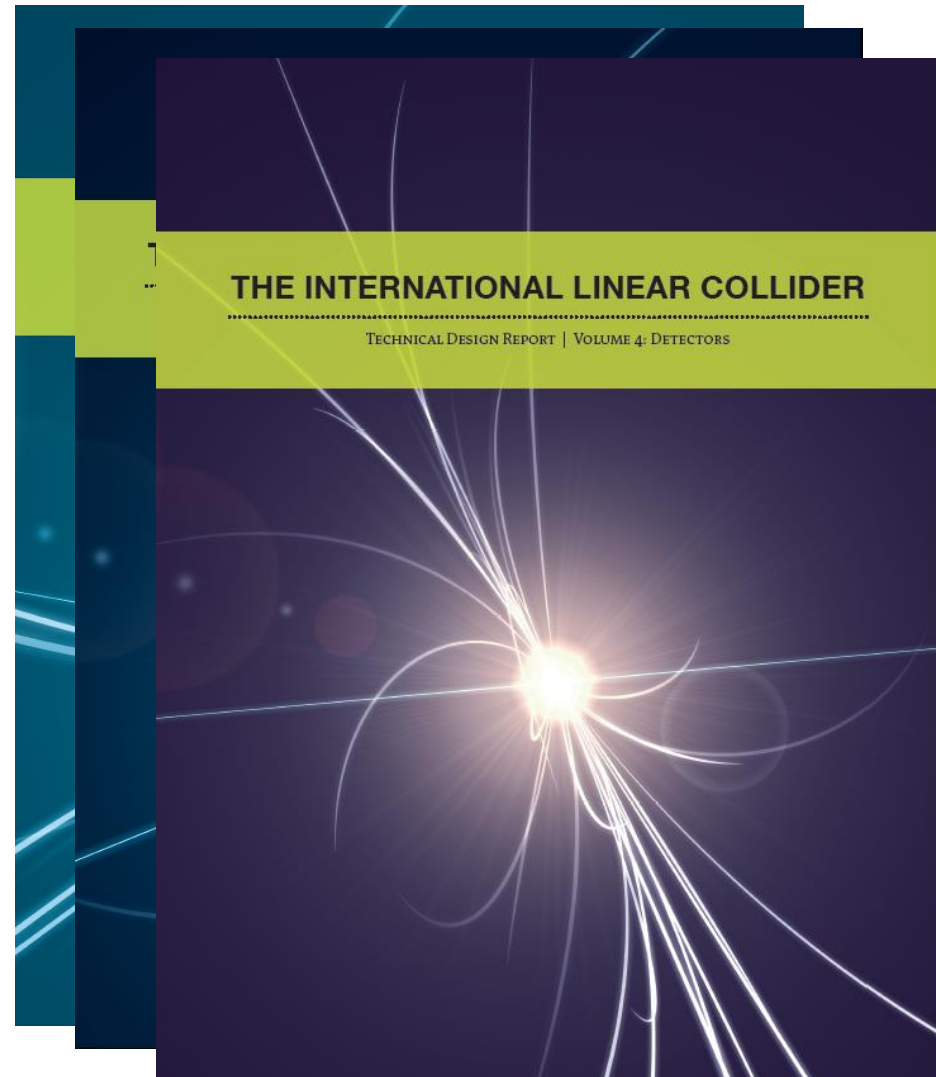
Gaugino Mass Measurement as Benchmark for a Particle Flow Detector at the ILC

Mikael Berggren, Jenny List,
Madalina Chera

LC Forum, DESY, 9-11 October 2013

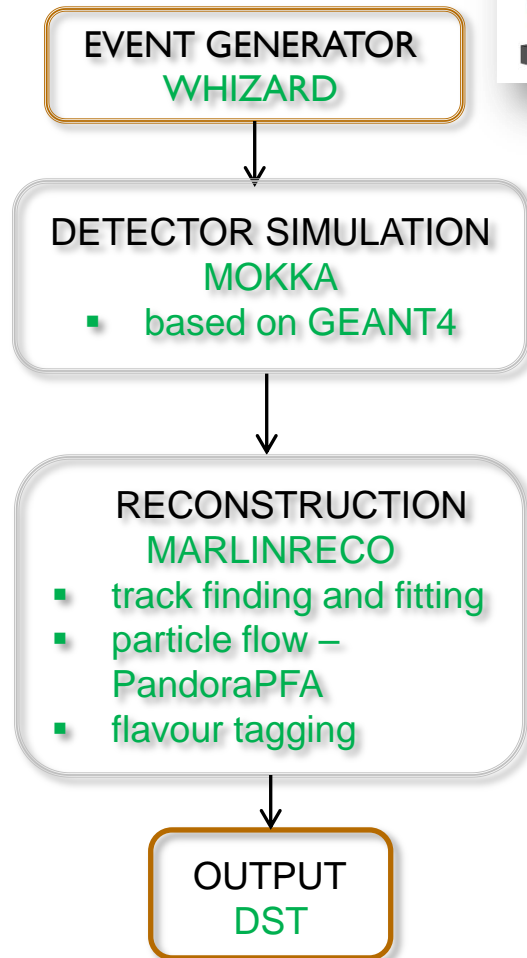
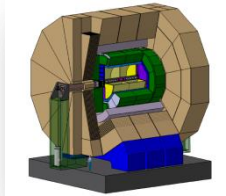
Motivation

- The ILC detector design optimisation & the physics studies are carried out with **a detector simulation**.
- The **Particle Flow** concept is very important for achieving the desired precision at the ILC.
- The PFlow is a crucial part of the reconstruction software.
- Due to the inherent changes and development of the software it is worthwhile to:
 - Quantify (parametrise) its performance
 - Study, compare and document the simulation and reconstruction performance of the available ILC simulations
 - Understand what could be improved in the detector design and reconstruction

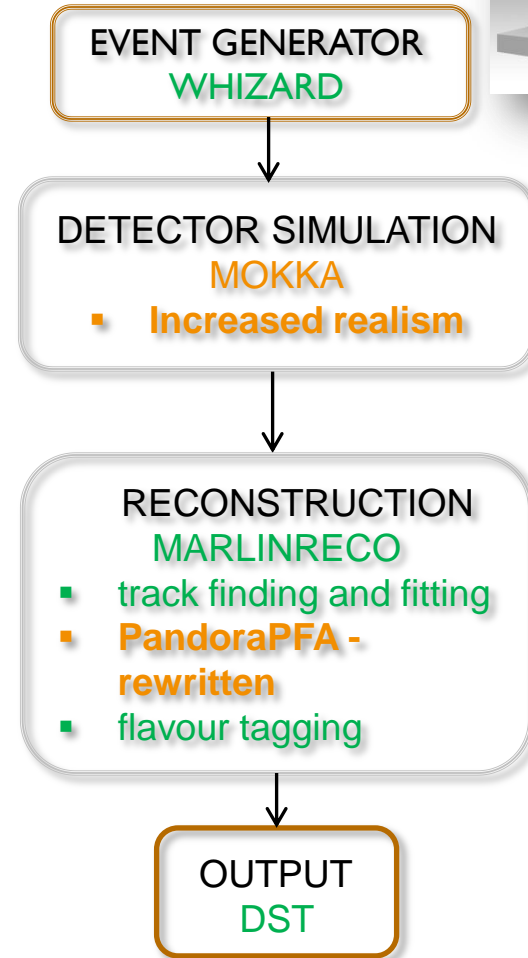
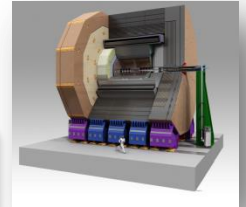


Current Detector Simulations

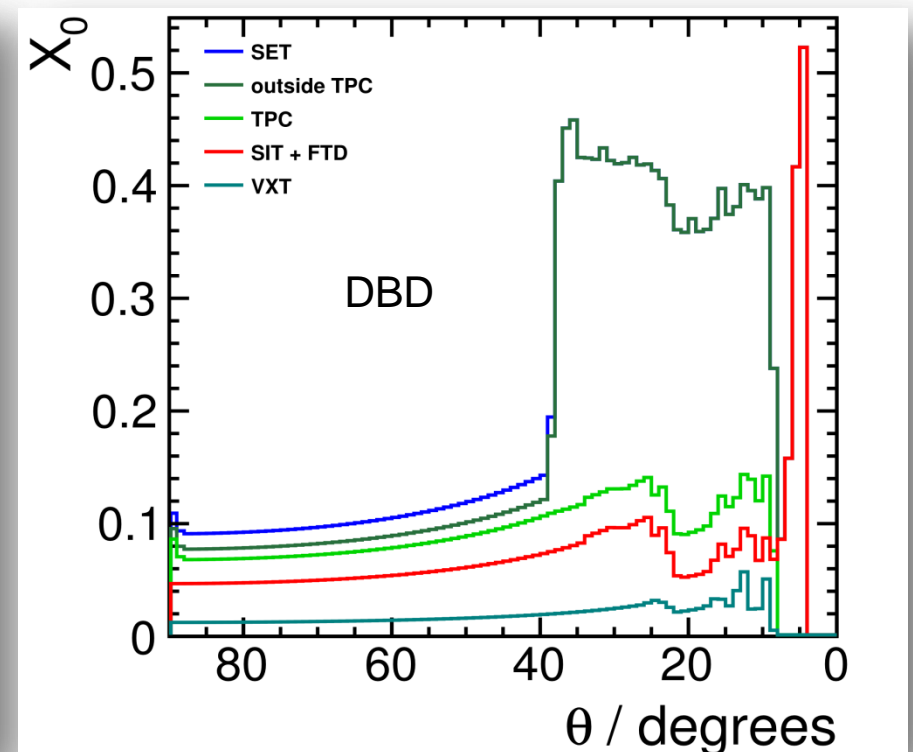
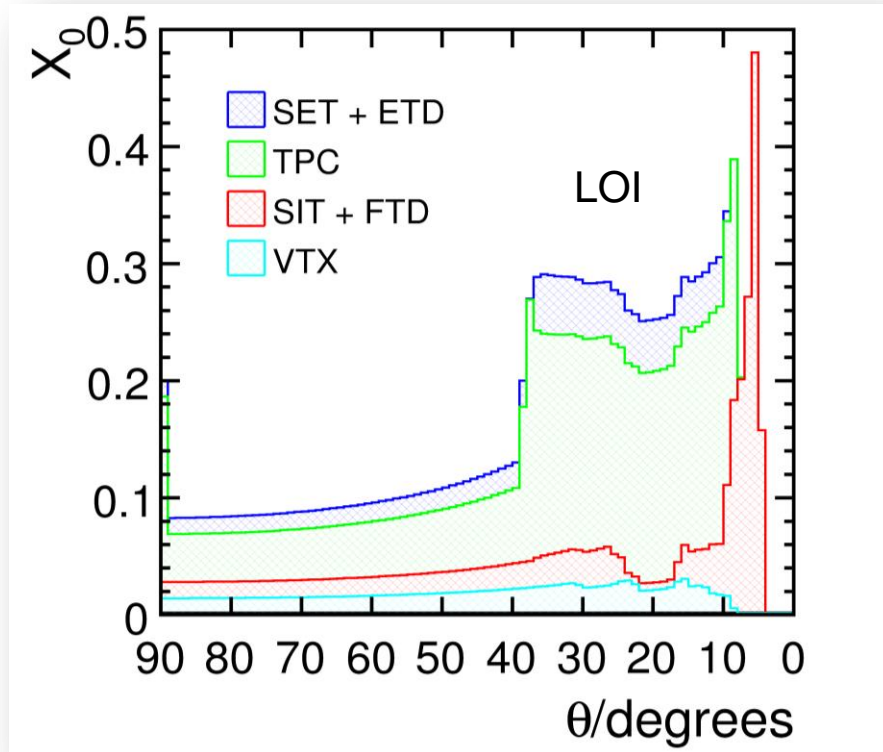
> Full Sim – „LOI“



> Full Sim – „DBD“



Changes Between LOI and DBD



> The new simulation → **improved detector realism:**

- the vertexing
- the tracker (TPC)
- the calorimeter

now include electronics and service materials.

Changes Between LOI and DBD

- > New forward tracking pattern recognition
- > New TPC pattern recognition
- > Pandora PFANew has been developed and rewritten

For $|\cos(\theta)| < 0.7$:

Jet Energy [GeV]	σ_{Ej}/E_j [LOI]	σ_{Ej}/E_j [DBD]
45	3.71 ± 0.05 %	3.66 ± 0.05 %
100	2.95 ± 0.04 %	2.83 ± 0.04 %
180	2.99 ± 0.04 %	2.86 ± 0.04 %
250	3.17 ± 0.05 %	2.95 ± 0.04 %

The jet energy resolution has actually improved despite the material addition.
Goal: **study what happens in a physics scenario!**

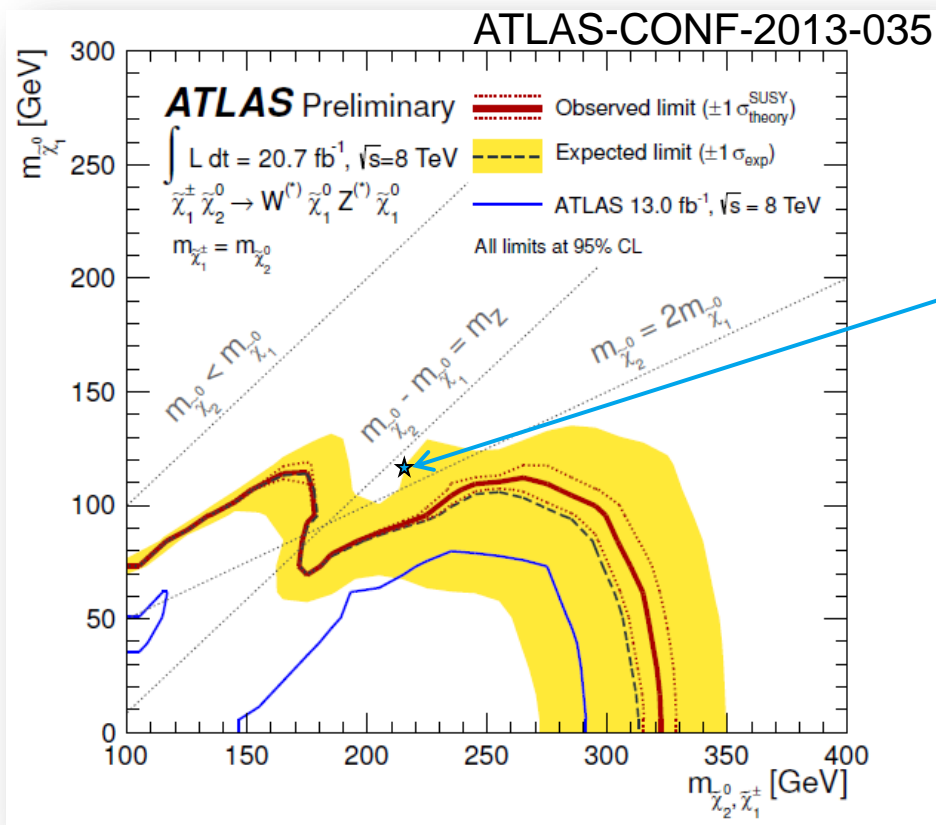


Study case: $\tilde{\chi}_1^\pm$ and $\tilde{\chi}_2^0$ Pair Production at the ILC

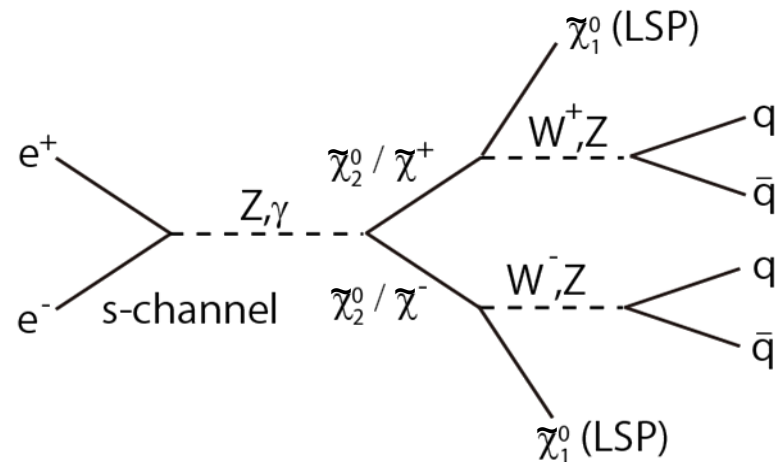
“Point 5” benchmark : gaugino pair production at ILC

<http://arxiv.org/pdf/1006.3396.pdf> (ILD Lol)

<http://arxiv.org/pdf/0911.0006v1.pdf> (SiD Lol)



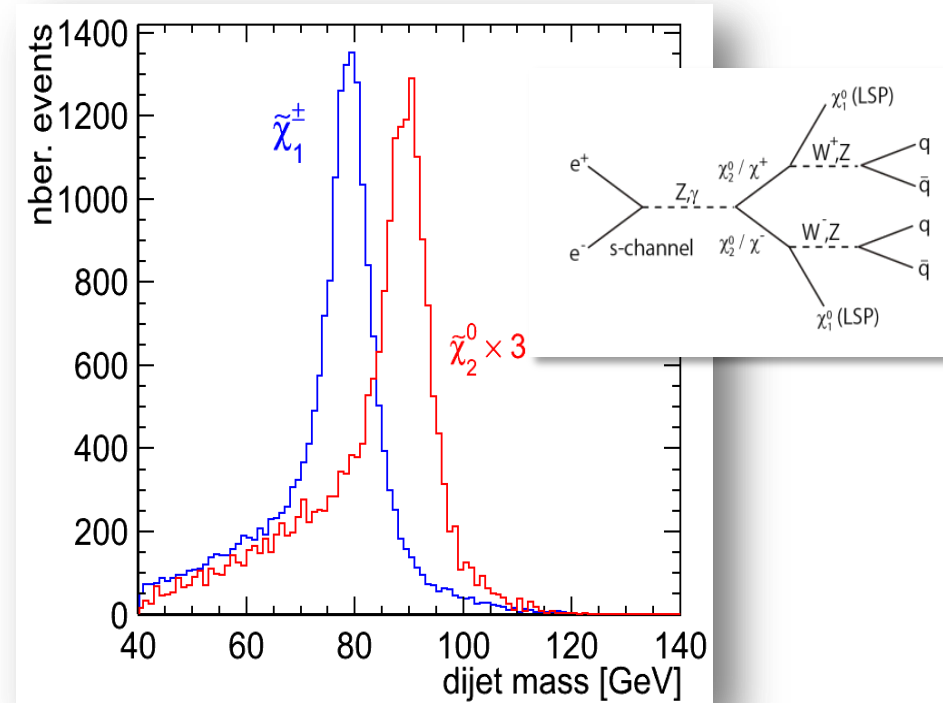
Particle	Mass [GeV]
$\tilde{\chi}_1^0$	115.7
$\tilde{\chi}_1^\pm$	216.5
$\tilde{\chi}_2^0$	216.7
$\tilde{\chi}_3^0$	380



Study case - motivation

- > The „point 5“ scenario is a good case for:
- > studying the detector and particle flow performance

- 2 escaping LSP's \rightarrow missing energy
 - hadronic decay of gauge bosons
 - goal: clearly distinguish between W and Z pair events
-
- > comparing and studying the performance of two versions of detector simulation (e.g. LOI and DBD)



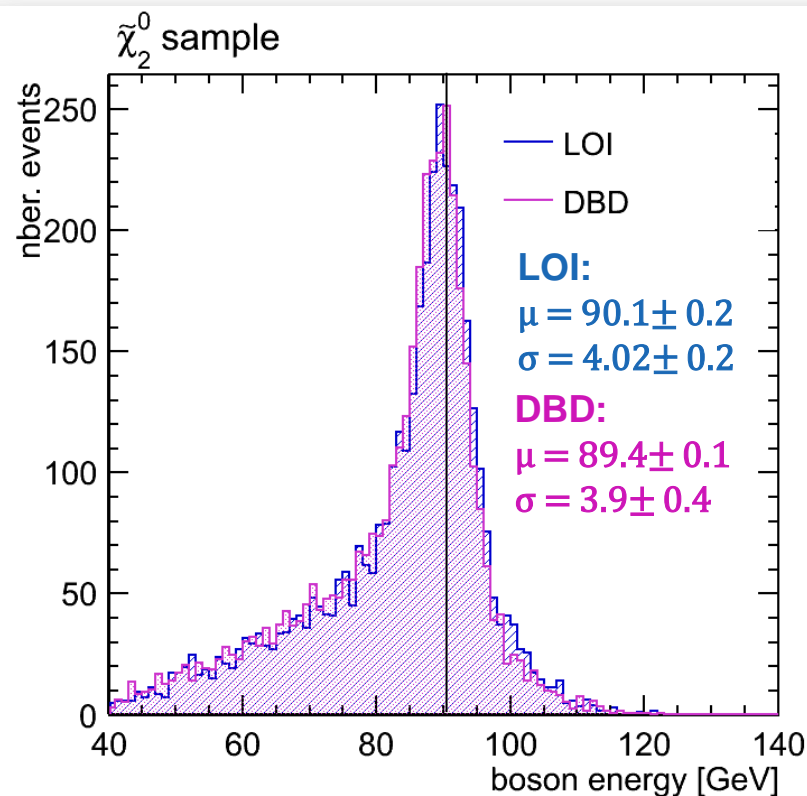
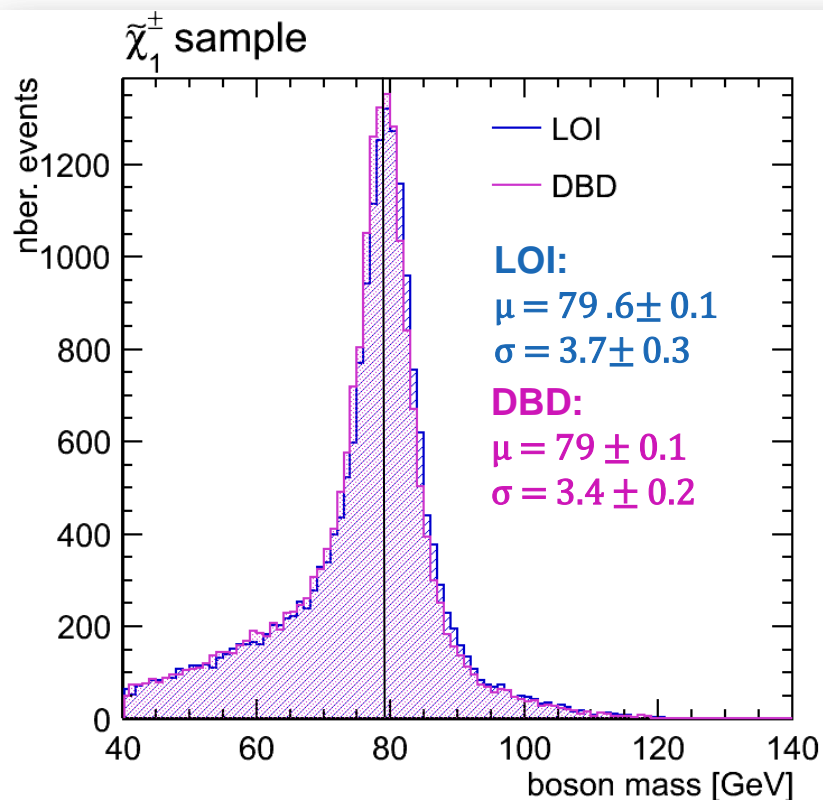
Study case – Analysis Flow

- > The **fully hadronic** decay modes of the on shell gauge bosons were chosen as **signal**
- > **Signal topology**: 4 jets and missing energy
- > **Background**:
 - SM 4f background is dominant
 - Each signal channel acts as background to the other!
- > Event **preselection** – apply cuts on:
 - Number of tracks in event and per jet
 - Minimum number of PFOs per jet = 3
 - Minimum jet energy and $|\cos(\theta)_{\text{jet}}|$
 - $|\cos(\theta)_{\text{pmiss}}| < 0.99$
 - $100 \text{ GeV} < E_{\text{visible}} < 300 \text{ GeV}$
 - $M_{\text{missing}} > 220 \text{ GeV}$
- > Perform **kinematic fit** using Marlin KinFit: equal mass constraint (determine best jet pairing)
 - Apply cut on converged kinematic fit



Dijet [Boson] Mass Comparison – LOI to DBD

> Use dijet mass to separate $\tilde{\chi}_1^\pm$ and $\tilde{\chi}_2^0$ events → measure cross section



> The DBD distribution appears slightly narrower and shifted towards lower energy, however the DBD and LOI distributions are compatible with each other.

$\tilde{\chi}_1^\pm$ and $\tilde{\chi}_2^0$ Mass Measurement

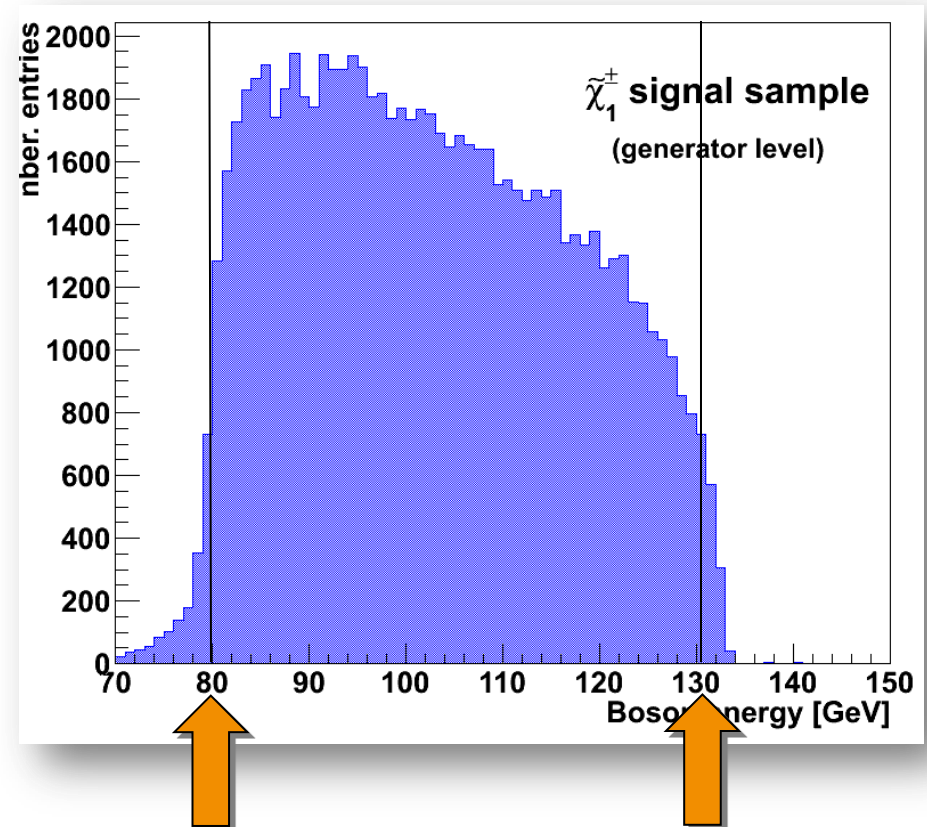
- > Mass difference to LSP ($\tilde{\chi}_1^0$) is **larger** than M_Z
- > Observe the decays of real gauge bosons
- > 2 body decay \rightarrow the edges of the energy spectrum are kinematically determined
- > **Use dijet energy spectrum „end points“ in order to calculate masses**

$$\gamma = \frac{E_{beam}}{M_\chi}$$

$$E_\pm = \gamma \cdot E_V^* \pm \gamma \cdot \beta \cdot \sqrt{E_V^{*2} - M_V^2}$$

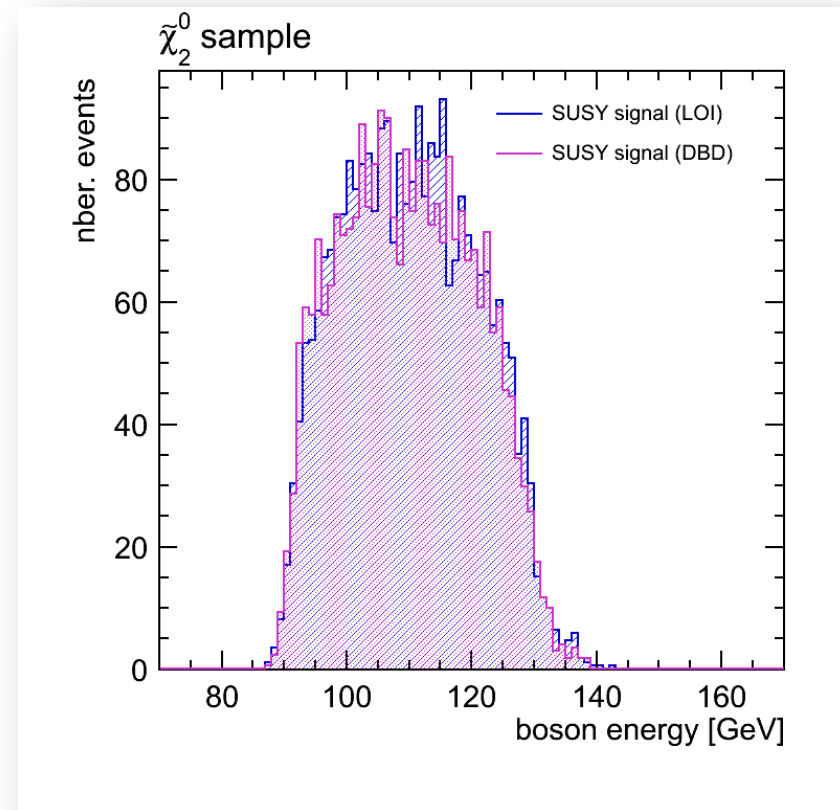
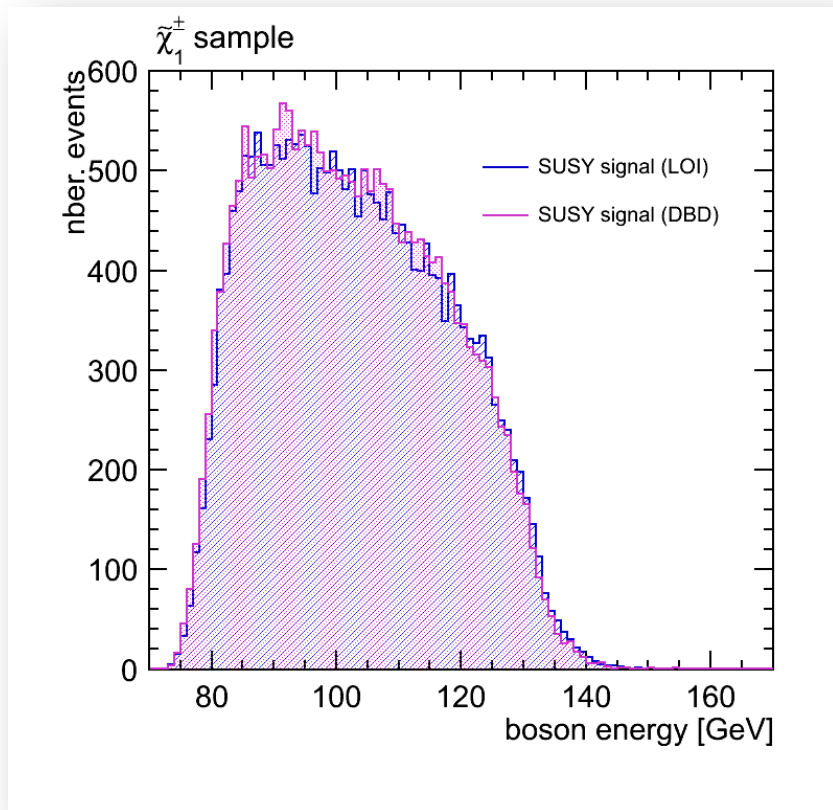
Real edge values [GeV]:

W_{low}	W_{high}	Z_{low}	Z_{high}
80.17	131.53	93.24	129.06



Dijet [Boson] Energy Comparison LOI - DBD

> Use dijet energy to measure $\tilde{\chi}_1^\pm$ and $\tilde{\chi}_2^0$ mass



> The DBD distribution appears slightly narrower and shifted towards lower energies. Nevertheless, **the two distributions agree very well.**

$\tilde{\chi}_1^\pm$ and $\tilde{\chi}_2^0$ Signal Sample Further Separation

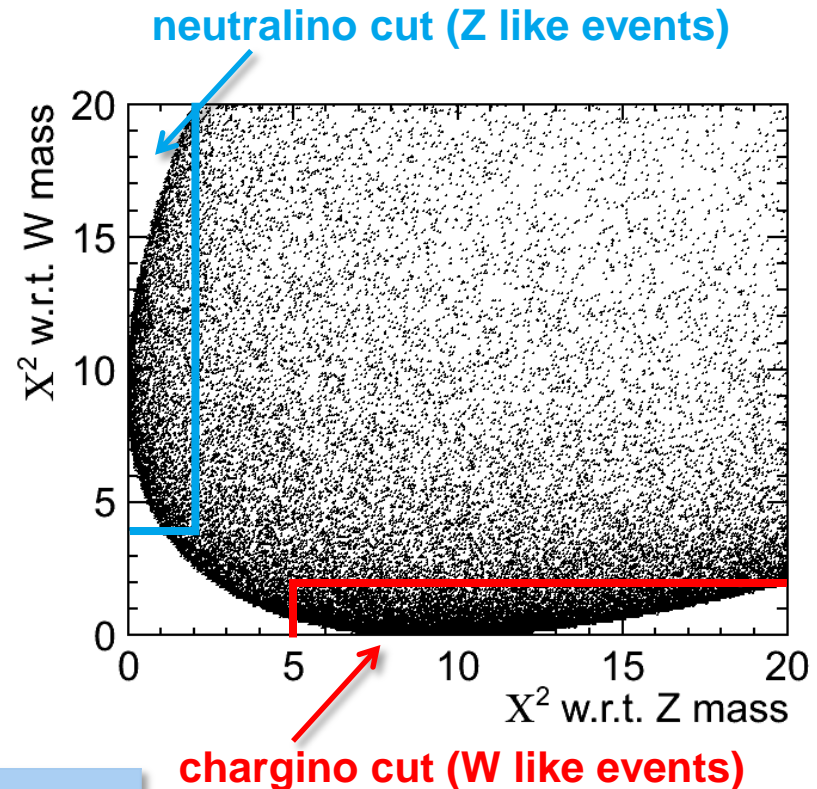
- > Calculate χ^2 with respect to nominal W / Z mass

$$\chi^2(m_{j1}, m_{j2}) = \frac{(m_{j1} - m_V)^2 + (m_{j2} - m_V)^2}{\sigma^2}$$



min $\chi^2 \rightarrow \tilde{\chi}_1^\pm$ and $\tilde{\chi}_2^0$ separation

- > Downside: lose statistics
 - Cut away 43% of $\tilde{\chi}_1^\pm$ surviving events
 - Cut away 68% of $\tilde{\chi}_2^0$ surviving events
- > However, after the χ^2 cut, the separation is quite clear:

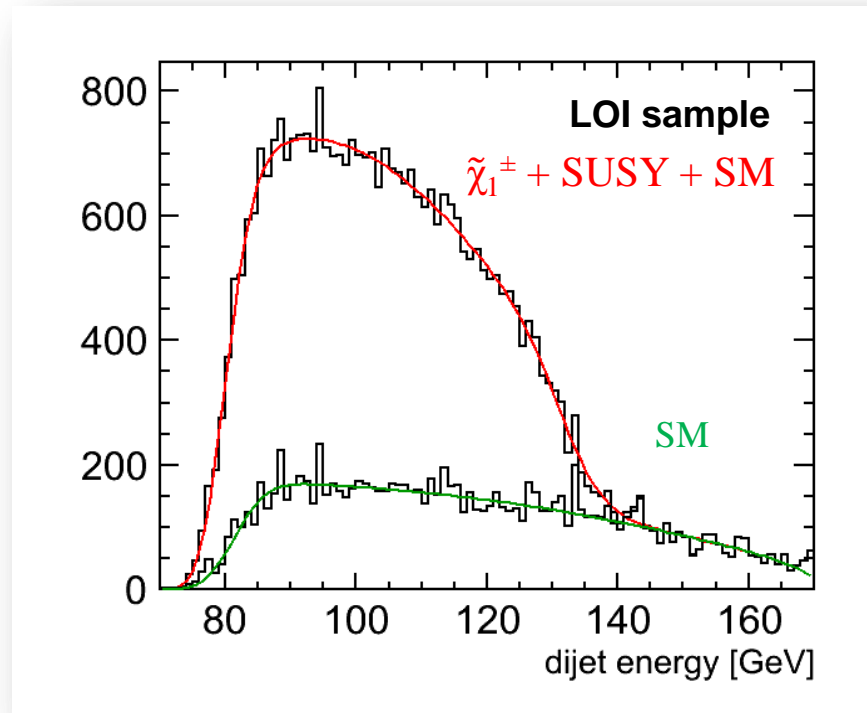


Obs.	DBD		LOI	
	$\tilde{\chi}_1^\pm$	$\tilde{\chi}_2^0$	$\tilde{\chi}_1^\pm$	$\tilde{\chi}_2^0$
Efficiency	57%	32%	56%	34%
Purity (total)	63%	35%	62%	35%
Purity (SUSY)	94%	68%	95%	66%

$\tilde{\chi}_1^\pm$ and $\tilde{\chi}_2^0$ Mass Measurement – “Endpoint” Method

- Fit dijet energy spectrum and obtain edge positions:

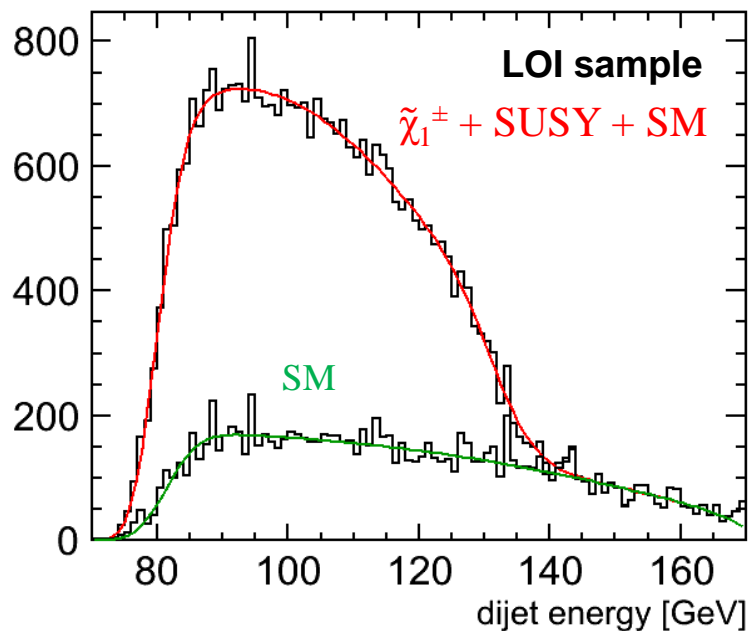
$$f(x; t_0, b_0, \sigma_1, \gamma) = f_{SM} + \int_{t_0}^{t_1} (b_2 t^2 + b_1 t + b_0) V(x - t, \sigma(t), \gamma) dt$$



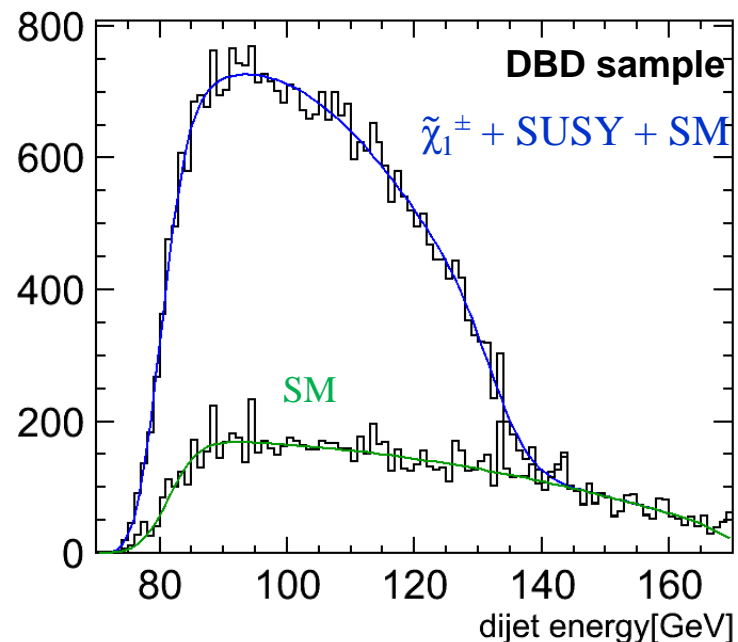
Where:

- The polynomial accounts for the slope of the initial spectrum
- The Voigt function accounts for the detector resolution and gauge boson width

Endpoint Extraction Comparison – LOI to DBD



$$E_{\text{low}} \simeq 79.7 \pm 0.3 \text{ GeV}$$
$$E_{\text{high}} \simeq 131.9 \pm 0.9 \text{ GeV}$$

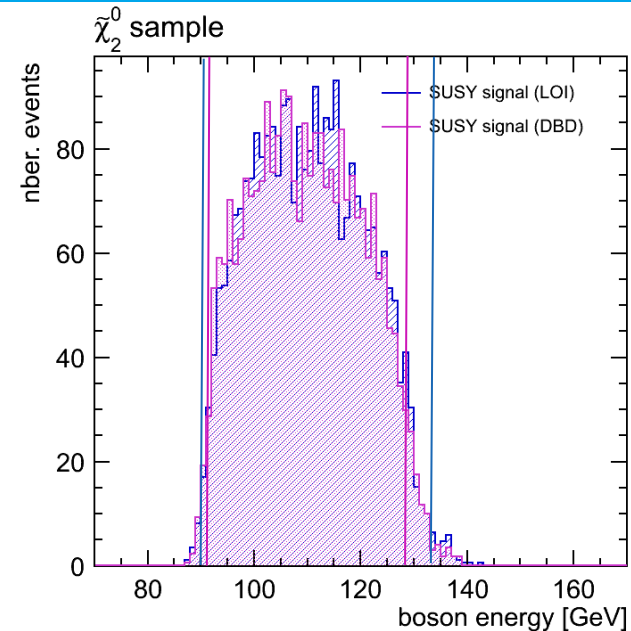
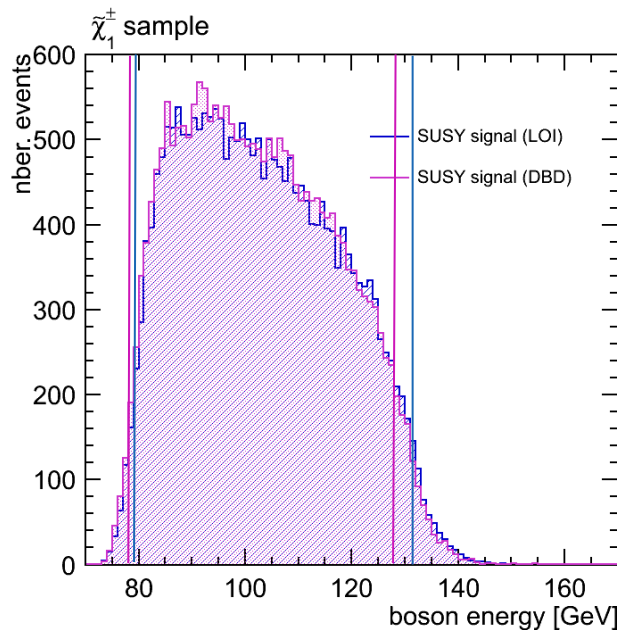


$$E_{\text{low}} \simeq 79.5 \pm 1.7 \text{ GeV}$$
$$E_{\text{high}} \simeq 128.3 \pm 1.2 \text{ GeV}$$

- > The DBD distribution appears slightly shifted towards lower energies. Nevertheless, **the two distributions agree very well.**



Issues of the „Endpoint Method“



Sim.	Edge W_{low} [GeV]	Edge W_{high} [GeV]	Edge Z_{low} [GeV]	Edge Z_{high} [GeV]
DBD	79.5 ± 1.7	128.3 ± 1.2	91.9 ± 0.8	127.9 ± 0.7
LOI	79.7 ± 0.3	131.9 ± 0.9	91.0 ± 0.7	133.6 ± 0.5

The fitting method appears to be highly dependent on small changes in the fitted distribution → it is clearly NOT appropriate for a comparing the simulation and reconstruction performance.

We need to apply a different edge extraction method!

Endpoint Extraction using an FIR Filter

- Finite Impulse Response (FIR) filters are digital filters used in signal processing.
- FIR filters can operate both on discrete as well as continuous values.
- The concept of “finite impulse response” ↔ **the filter output** is computed as a finite, weighted sum of a finite number of values from the filter input.

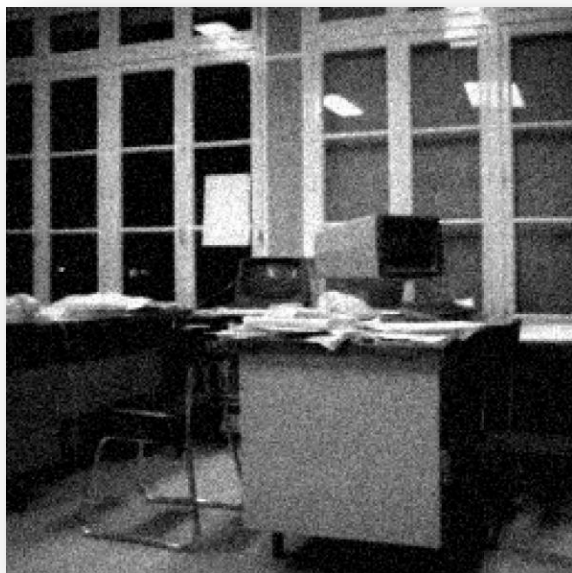
$$y[n] = \sum_{k=-M_1}^{M_2} b_k x[n-k]$$

the input signal

the filter coefficients (weights)

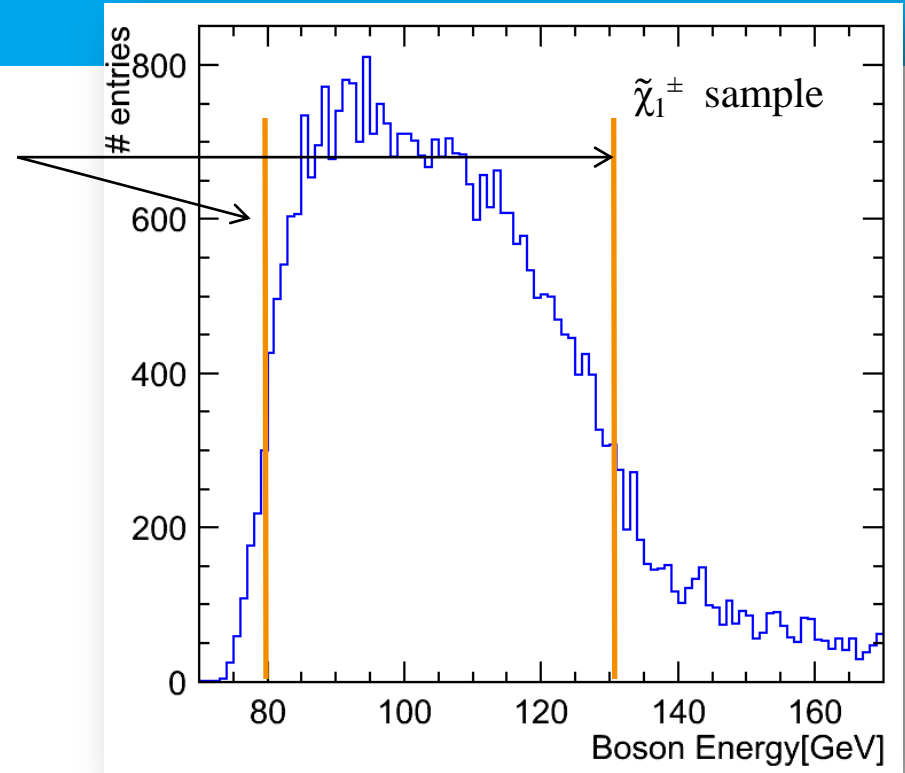
- y is obtained by convolving the input signal with the (finite) weights
- FIR filters are used to detect edges in image processing techniques:

D. Demigny, T. Kamlé



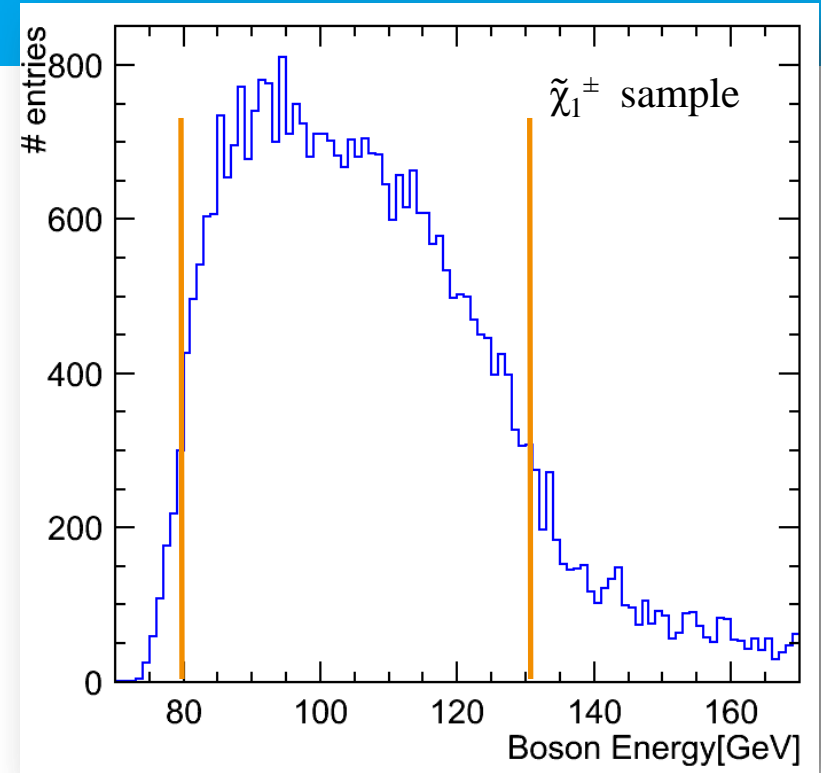
Applying an FIR Filter

- > Goal: find edge positions in spectrum
- > Strategy: use weighted sums of bin content values to find patterns in distribution



Applying an FIR Filter

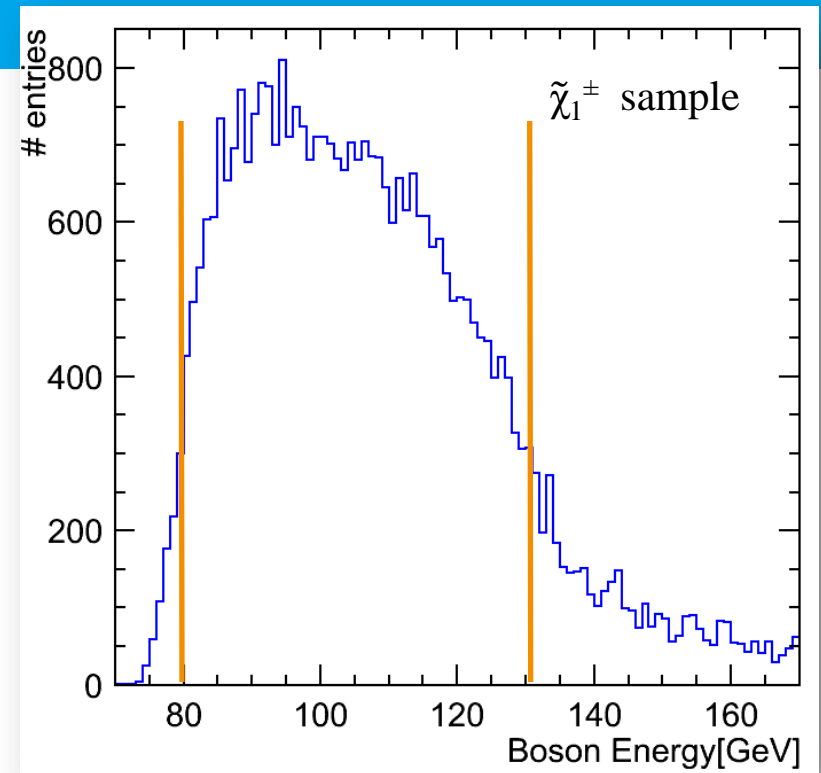
- > Goal: find edge positions in spectrum
- > Strategy: use weighted sums of bin content values to find patterns in distribution
- > Consider the histogram as an array of bin content values



Bin #	1	2	3	...	98	99	100
Entries	0	15	28	...	34	22	4

Applying an FIR Filter

- > Goal: find edge positions in spectrum
- > Strategy: use weighted sums of bin content values to find patterns in distribution
- > Consider the histogram as an array of bin content values
- > Consider an array of chosen weights (smaller than the histogram!)
- > Create new array of the same size:
 - Each entry in the new array is the weighted sum of the bin content values from the bins surrounding the corresponding bin in the original array.
 - The array is filled using the **same** (finite) weights each time.
- > The value of the output depends on the pattern in the neighbourhood of the considered bin and NOT on the position of the bin
- > The pattern of weights = kernel
- > The filter application = convolution



Bin #	1	2	3	...	98	99	100
Entries	0	15	28	...	34	22	4

$$w_1 \times 0 + w_2 \times 15 + w_3 \times 28 = \text{val2}$$

Entries	val1	val2	val3	...	val98	val99	val100
---------	------	------	------	-----	-------	-------	--------

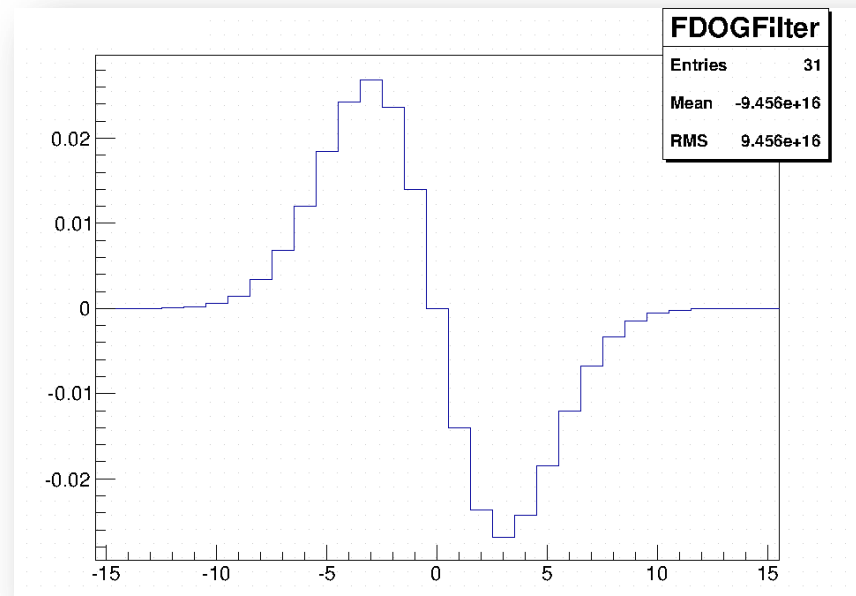


Choosing the Appropriate Filter

- > Idea: first derivative as kernel → it works but may be rather noisy
- > In order to choose an appropriate filter one can apply the following criteria:

Canny's criteria: [J. F. Canny. **A computational approach to edge detection.** *IEEE Trans. Pattern Analysis and Machine Intelligence*, pages 679-698, 1986]

- Good detection: probability of obtaining a peak in the response must be high
 - Localisation: standard deviation of the peak position must be small
 - Multiple response minimisation: probability of false positive detection must be small
- > Canny has suggested that an optimal filter is very similar to the **first derivative of a Gaussian**



Testing the FDOG Filter

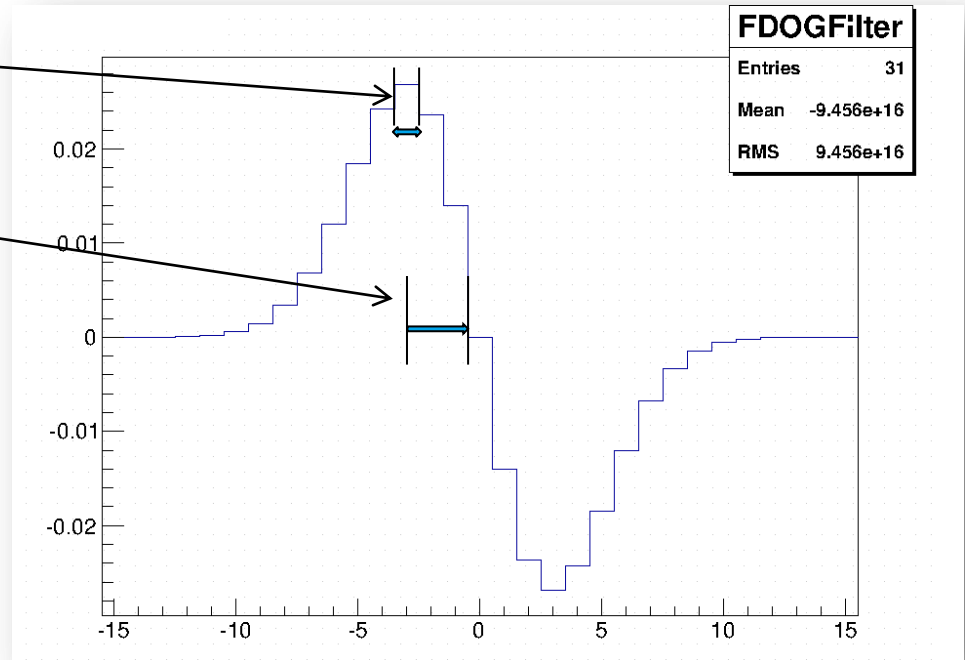
➤ There are two important filter characteristics that must be optimised:

the bin size

the filter size

It is crucial to strike the right balance between the two:

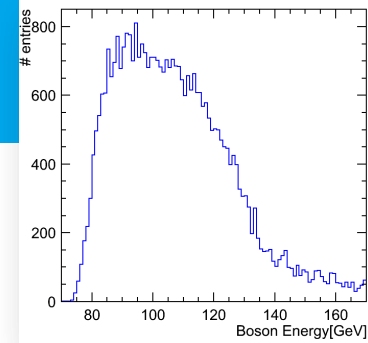
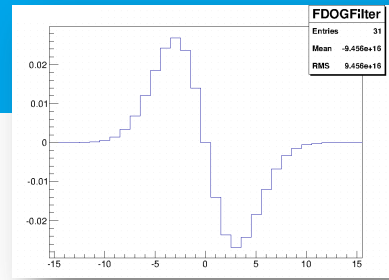
- If the bin size is too small → the filter picks up a lot of statistical fluctuations
- If the filter size is too large → the edge position cannot be localised anymore



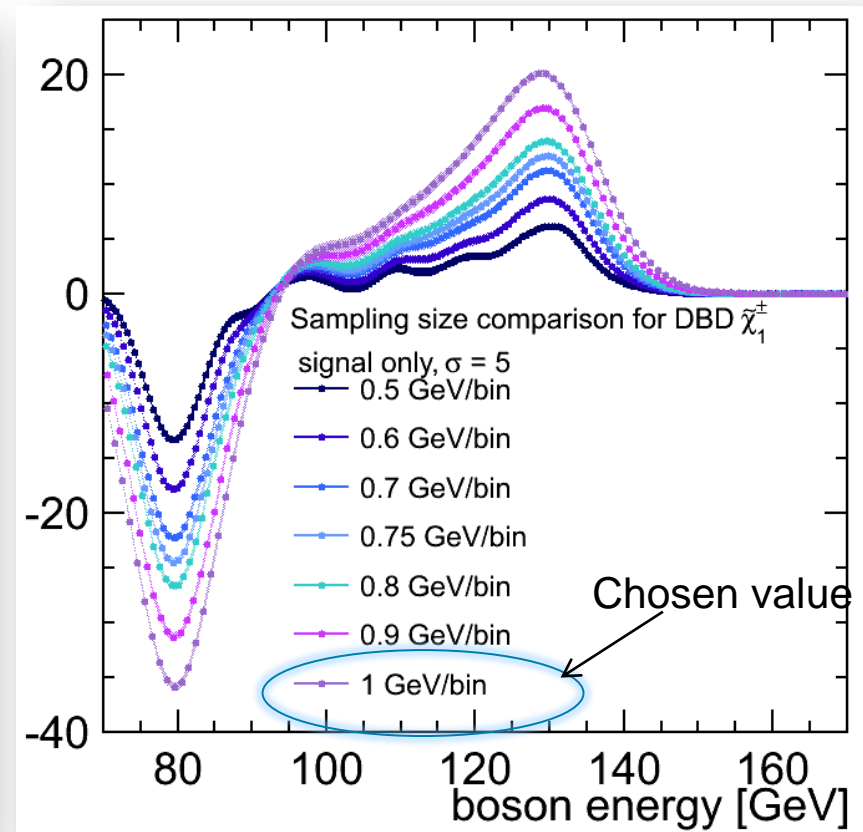
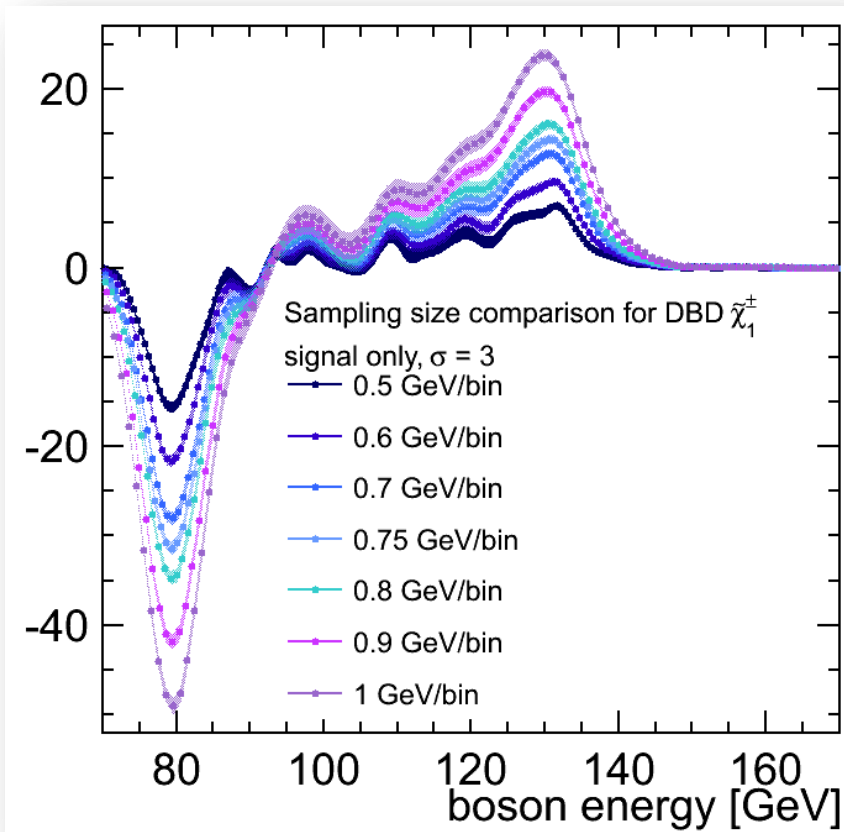
A toy MC study is needed to optimise the filter and bin size!

Testing the FDOG Filter

- > There are two important filter characteristics that must be optimised: the **bin size** and the filter size.



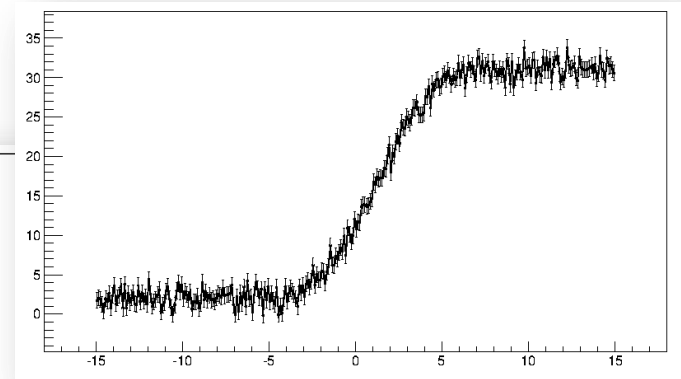
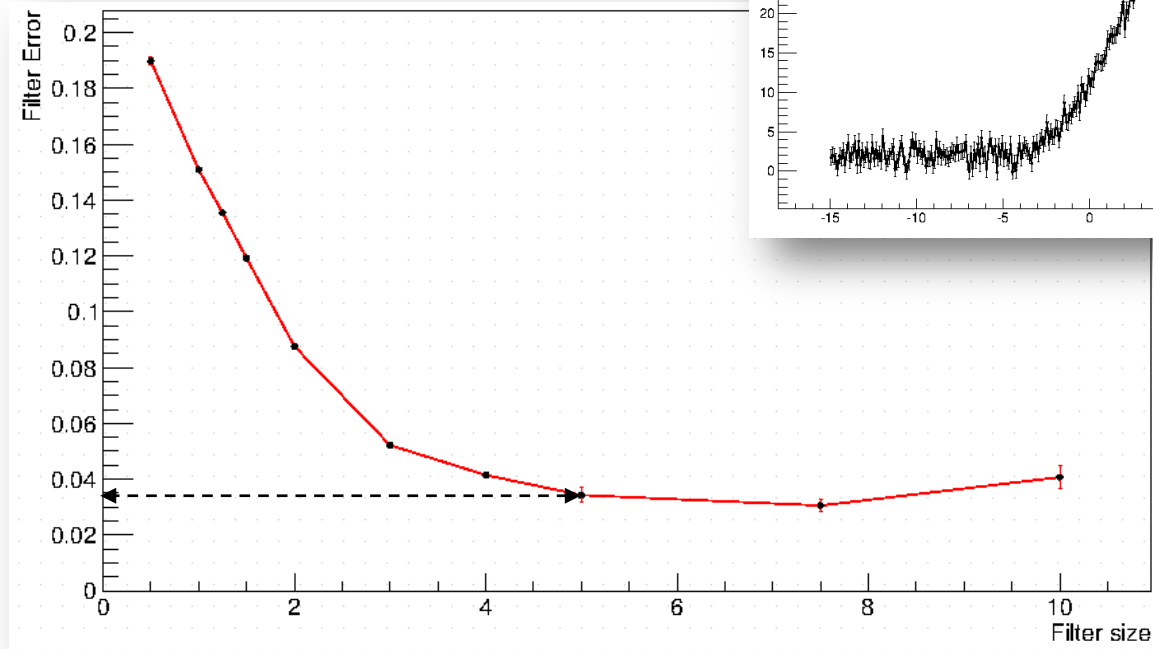
Filter response after applying the FDOG Filter to the $\tilde{\chi}_1^\pm$ energy distribution:



Testing the FDOG Filter

- > There are two important filter characteristics that must be optimised: the bin size and the **filter size**.
- > Filter size $\leftrightarrow \sigma$ of the FDOG kernel

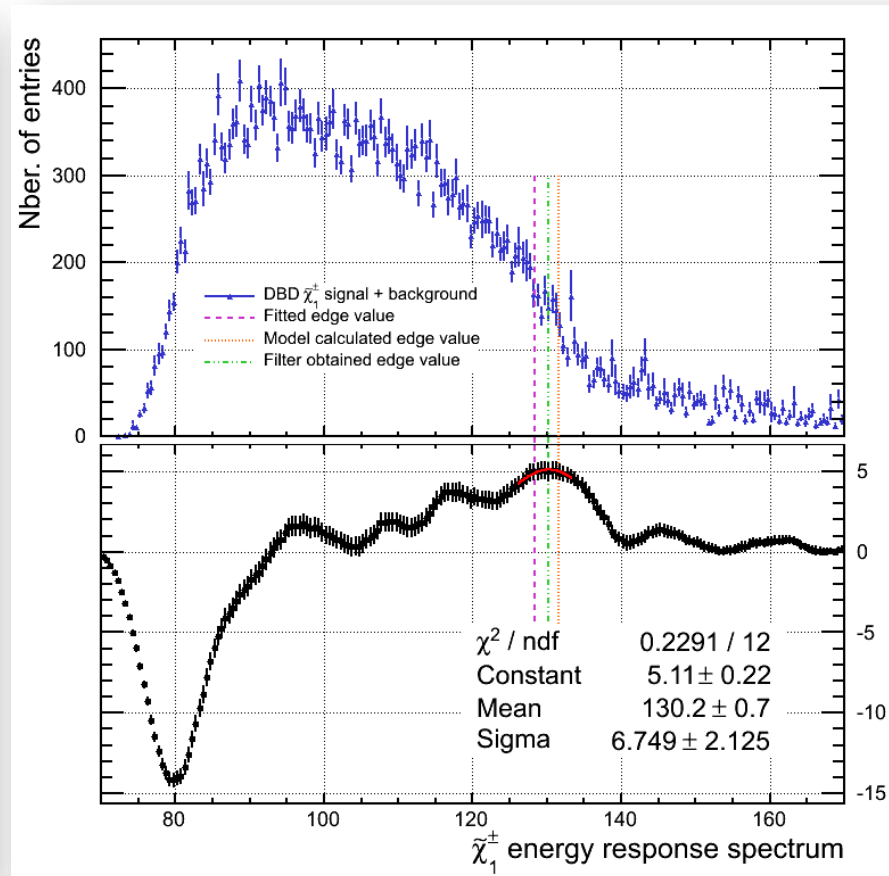
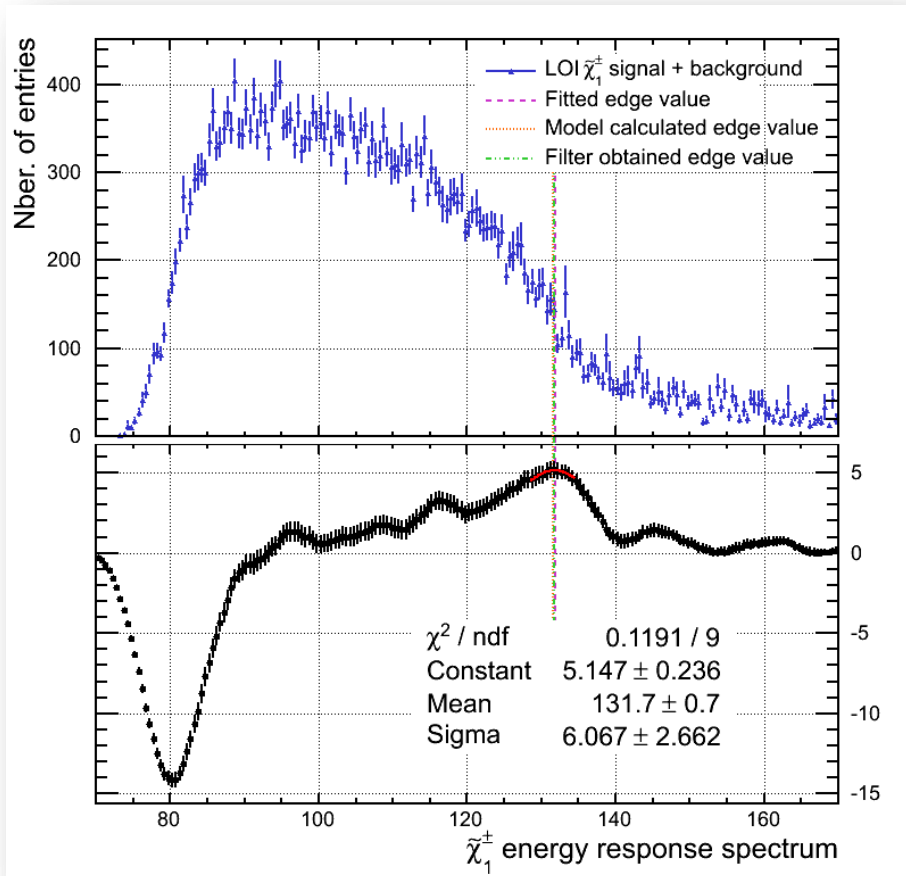
Studied the effect of the filter size on a smeared step edge monte carlo data.



S. Caiazza

The $\sigma = 5$ value filter size is very close to the minimum range of the error curve.

FIR Edge Extraction Comparison – LOI to DBD

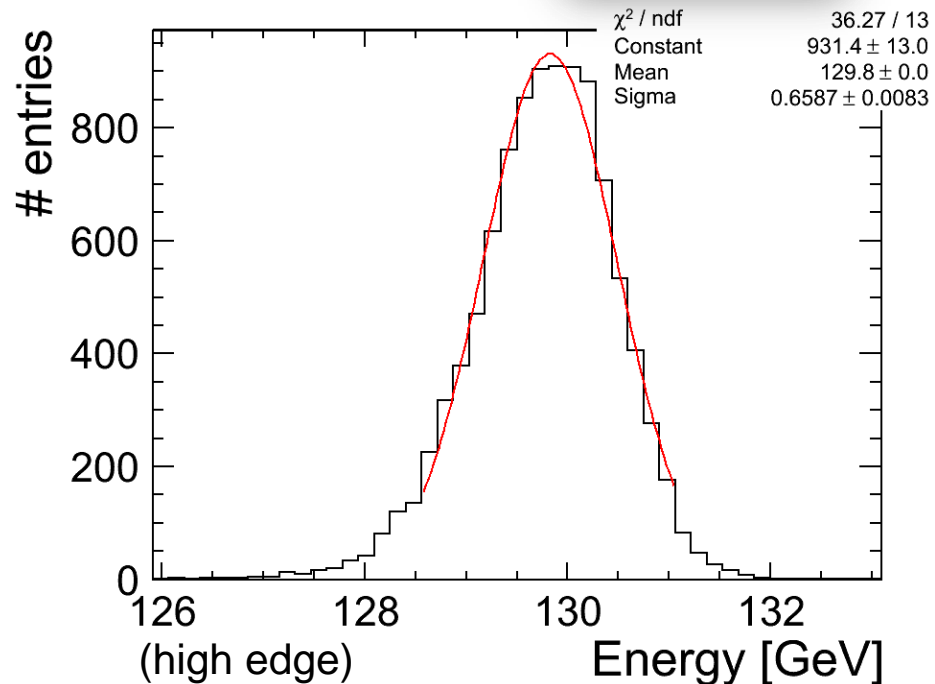
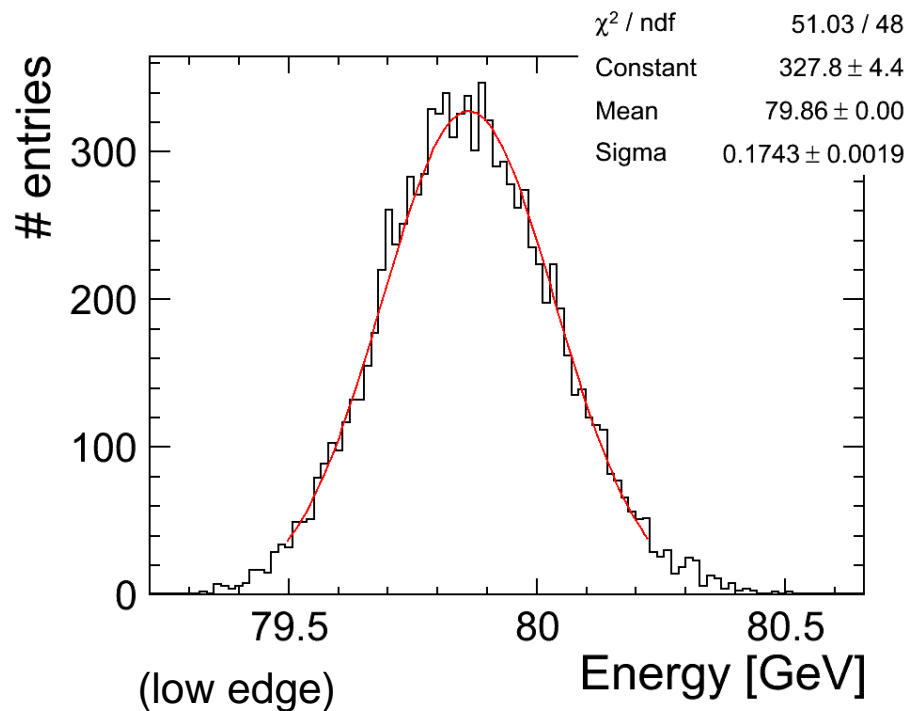
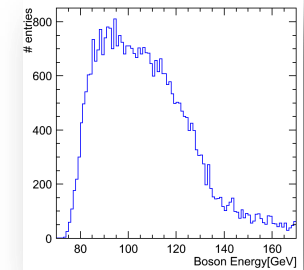


In the **LOI** case: the fitted and filter values are extremely close to the real model value.
In the **DBD** case: the filter value is much closer to the model one than the fitted edge.

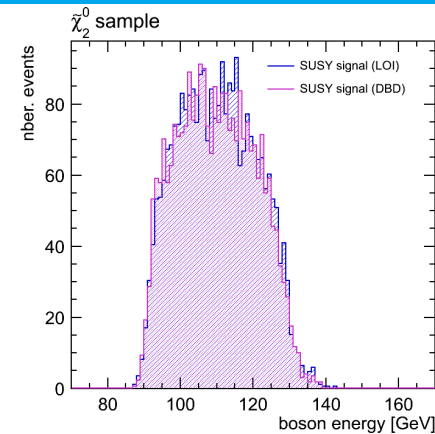
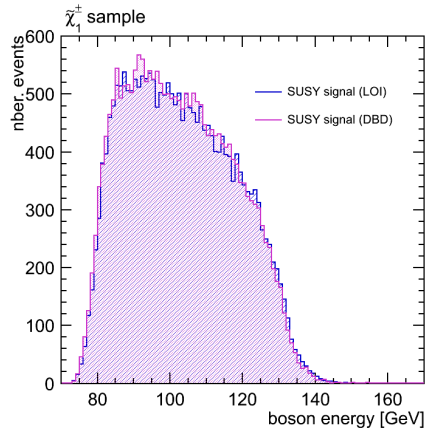


Toy MC for the Filter Edge Extraction

- To estimate the statistical precision of the edge extraction → toy MC
- 10000 $\tilde{\chi}_1^\pm$ and $\tilde{\chi}_2^0$ energy spectra have been produced
- The FDOG filter was then applied 10000 times
- Example: for the $\tilde{\chi}_1^\pm$ case:



Edge Extraction Comparison



True	80.17	131.53	93.24	129.06
Sim.	Edge W_{low} [GeV]	Edge W_{high} [GeV]	Edge Z_{low} [GeV]	Edge Z_{high} [GeV]
LOI	79.7 ± 0.3	131.9 ± 0.9	91.0 ± 0.7	133.6 ± 0.5
DBD	79.5 ± 1.7	128.3 ± 1.2	91.9 ± 0.8	127.9 ± 0.7
DBD filter	80.1 ± 0.2	129.1 ± 0.7	91.9 ± 0.2	127.2 ± 0.7

The filter extraction method is preferable:

- it is more stable
- provides smaller uncertainties in determining the edge position.

Conclusions

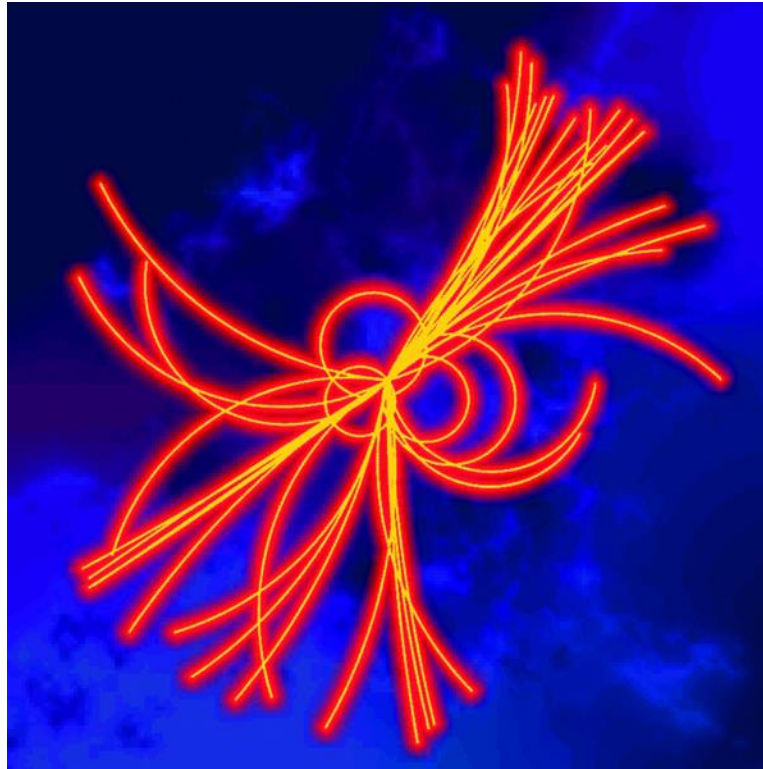
- It is important to study and compare the performance of our detector simulation and reconstruction software.
- The comparison should also be done within a physics scenario.
- The $\tilde{\chi}_1^\pm$ and $\tilde{\chi}_2^0$ pair production in the framework of the “Point 5” benchmark has been presented as study case.
- A preliminary comparison between the LOI and DBD simulation and reconstruction has been made;
 - The dijet mass reconstruction from the DBD is compatible to the LOI analysis.
 - The DBD reconstructed boson energy spectrum is very similar to the LOI one
 - However the fitting method for the mass determination appears very sensitive to small changes. A more robust method is needed.
 - Applying a finite impulse response (FIR) filter in order to extract the edge information instead of the fitting method is:
 - More robust (i.e. independent on distribution shape)
 - Provides just as good if not better statistical precision

> Outlook:

- A mass calibration will be performed for the mass measurement.



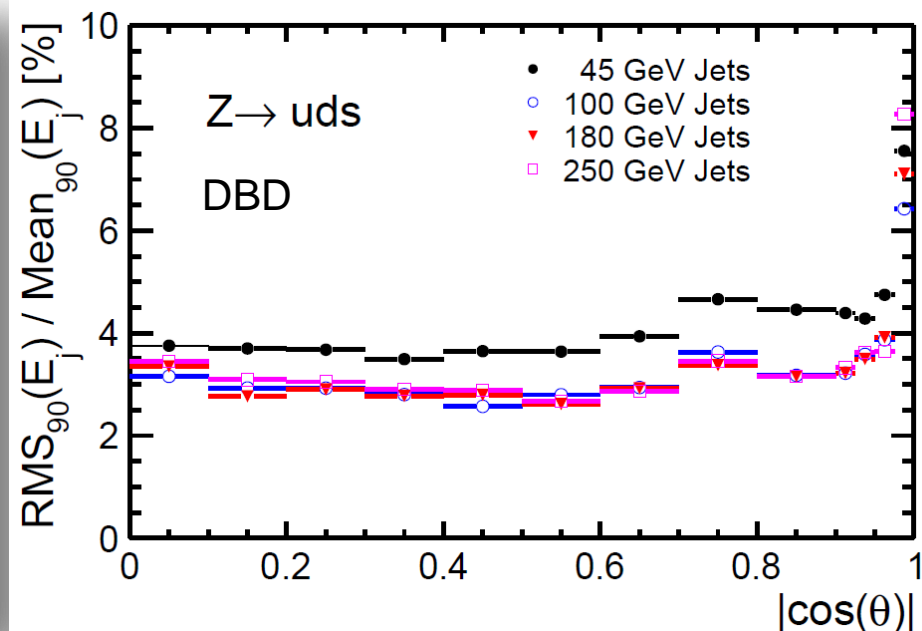
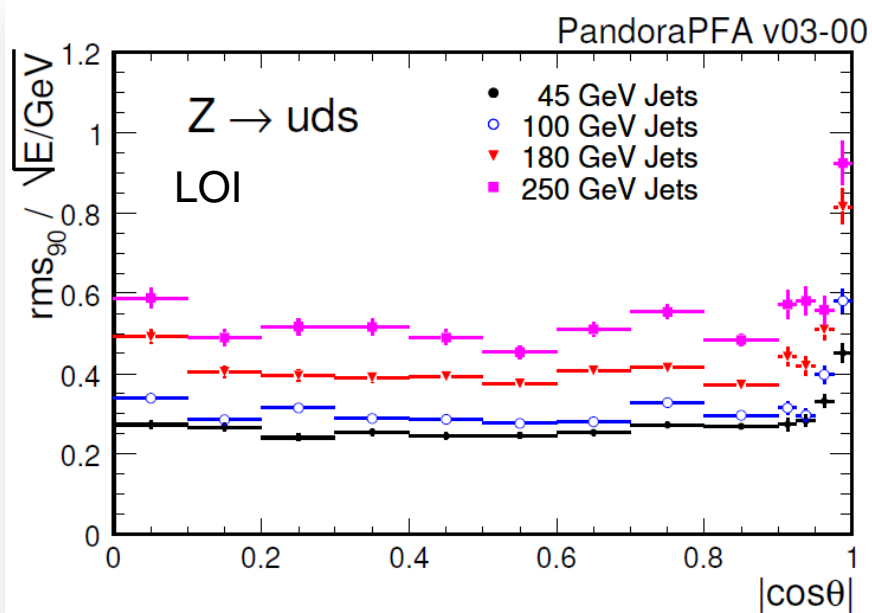
Thank You!



Back up



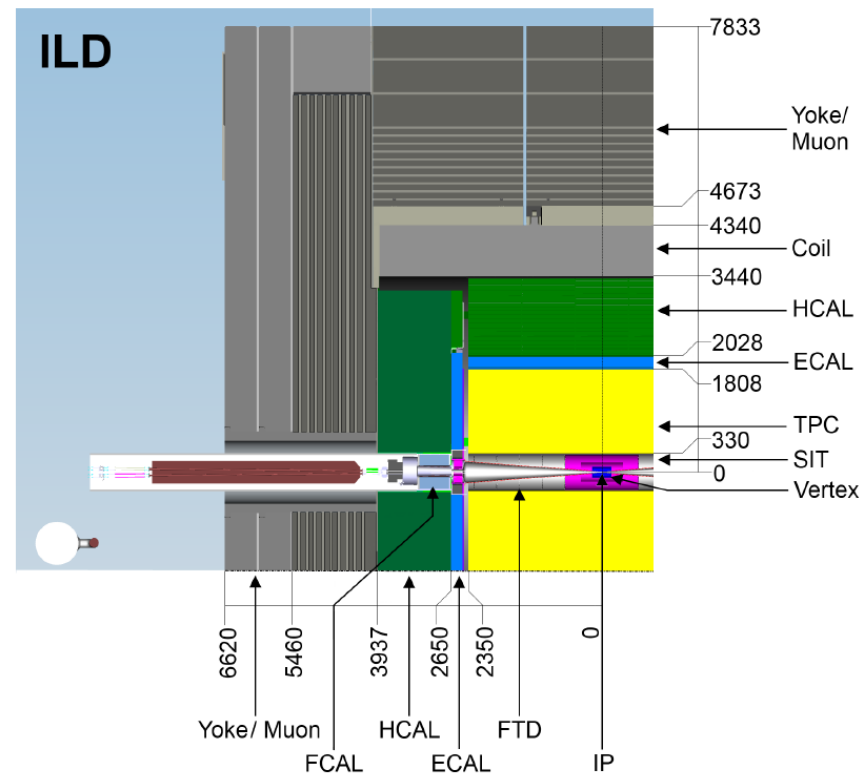
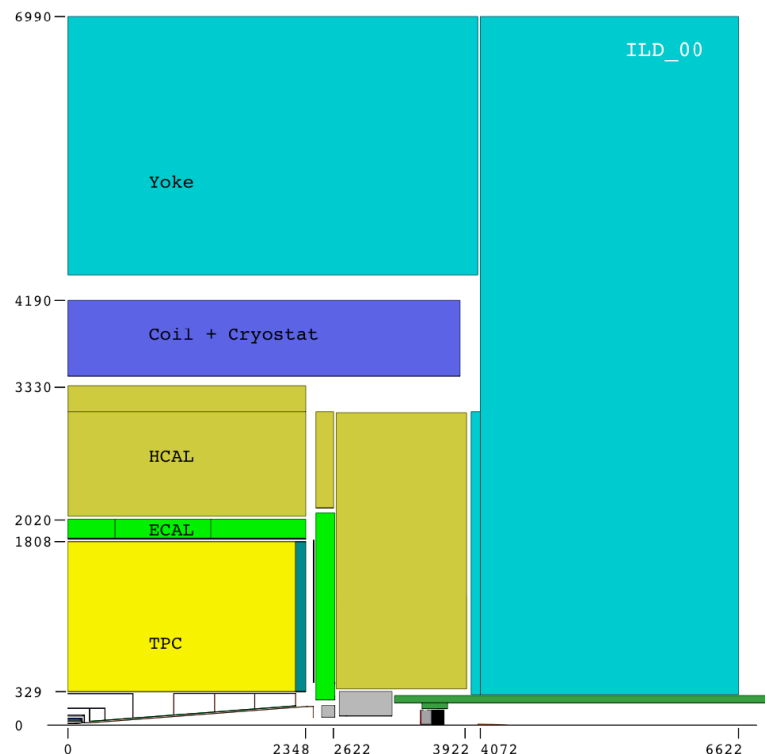
Changes Between LOI and DBD



➤ For $|\cos(\theta)| < 0.7$:

Jet Energy [GeV]	σ_{E_j}/E_j [LOI]	σ_{E_j}/E_j [DBD]
45	$3.71 \pm 0.05 \%$	$3.66 \pm 0.05 \%$
100	$2.95 \pm 0.04 \%$	$2.83 \pm 0.04 \%$
180	$2.99 \pm 0.04 \%$	$2.86 \pm 0.04 \%$
250	$3.17 \pm 0.05 \%$	$2.95 \pm 0.04 \%$

Changes Between LOI and DBD



> The new simulation → **improved detector realism:**

- the vertexing
- the tracker (TPC)
- the calorimeter

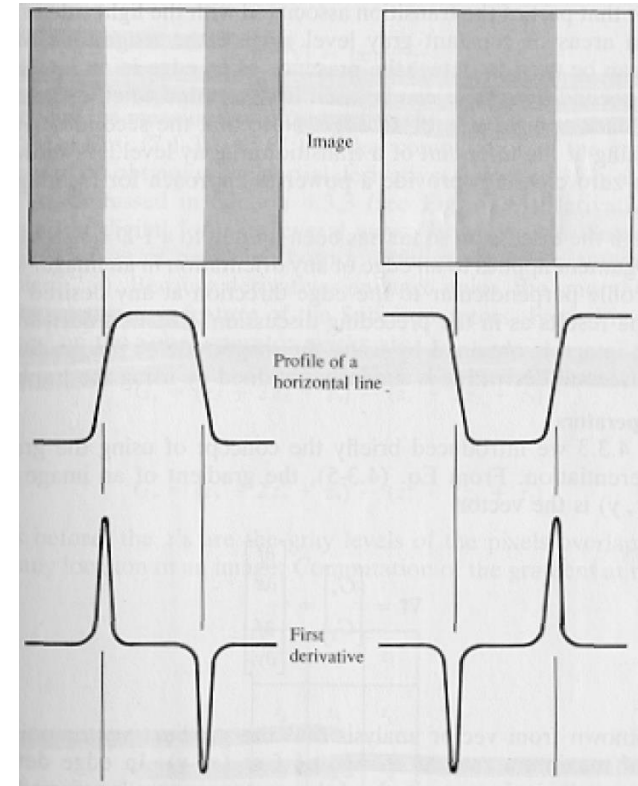
now include electronics and service materials.

Applying an FIR Filter – Example: the box function

- > The changes of a function can be described by the derivative → interpret the histogram as a 1D function
- > The points that lie on the edge of the distribution → detected by local maxima and minima of the first derivative

$$f'(x) = \lim_{h \rightarrow 0} \frac{f(x+h) - f(x)}{h} \approx f(x+1) - f(x) \quad (h = 1)$$

- > The first derivative is approximated by using the **kernel [-1, 0, 1]**



Applying an FIR Filter – Example: the box function

- > The changes of a function can be described by the derivative → interpret the histogram as a 1D function
- > The points that lie on the edge of the distribution → detected by local maxima and minima of the first derivative

$$f'(x) = \lim_{h \rightarrow 0} \frac{f(x+h) - f(x)}{h} \approx f(x+1) - f(x) \quad (h=1)$$

- > The first derivative is approximated by using the **kernel [-1, 0, 1]**
- > The kernel is convoluted with the histogram:

$$response_i = -1 \times bin_{i-1} + 0 \times bin_i + 1 \times bin_{i+1}$$

